

Discovery of an Orally Bioavailable Benzofuran Analogue that Serves as a β -amyloid Aggregation Inhibitor for the Potential Treatment of Alzheimer's Disease

Heejin Ha, Dong Wook Kang, Hyuk-Min Kim, Jin-Mi Kang, Jihyae Ann, Hyae Jung Hyun, Joon Hwan Lee, Sae Hee Kim, Hee Kim, Kwanghyun Choi, Hyun-Seok Hong, Young Ho Kim, Dong-Gyu Jo, Jiyoun Lee, and Jeewoo Lee

J. Med. Chem., **Just Accepted Manuscript** • DOI: 10.1021/acs.jmedchem.7b00844 • Publication Date (Web): 21 Nov 2017

Downloaded from <http://pubs.acs.org> on November 22, 2017

Just Accepted

"Just Accepted" manuscripts have been peer-reviewed and accepted for publication. They are posted online prior to technical editing, formatting for publication and author proofing. The American Chemical Society provides "Just Accepted" as a free service to the research community to expedite the dissemination of scientific material as soon as possible after acceptance. "Just Accepted" manuscripts appear in full in PDF format accompanied by an HTML abstract. "Just Accepted" manuscripts have been fully peer reviewed, but should not be considered the official version of record. They are accessible to all readers and citable by the Digital Object Identifier (DOI®). "Just Accepted" is an optional service offered to authors. Therefore, the "Just Accepted" Web site may not include all articles that will be published in the journal. After a manuscript is technically edited and formatted, it will be removed from the "Just Accepted" Web site and published as an ASAP article. Note that technical editing may introduce minor changes to the manuscript text and/or graphics which could affect content, and all legal disclaimers and ethical guidelines that apply to the journal pertain. ACS cannot be held responsible for errors or consequences arising from the use of information contained in these "Just Accepted" manuscripts.

Discovery of an Orally Bioavailable Benzofuran Analogue that Serves as a β -amyloid Aggregation Inhibitor for the Potential Treatment of Alzheimer's Disease

Hee-Jin Ha,^{‡,§} Dong Wook Kang,[†] Hyuk-Min Kim,[†] Jin-Mi Kang,[†] Jihyae Ann,[†] Hye Jung Hyun,^{||} Joon Hwan Lee,^{||} Sae Hee Kim,^{||} Hee Kim,[‡] Kwanghyun Choi,[‡] Hyun-Seok Hong,[‡] YoungHo Kim,[‡] Dong-Gyu Jo,[§] Jiyoun Lee,[⊥] Jeewoo Lee^{*,†}

[†] Laboratory of Medicinal Chemistry, College of Pharmacy, Seoul National University, 1 Gwanak-ro, Gwanak-gu, Seoul 08826, Republic of Korea

[‡] Medifron DBT, Sandanro 349, Danwon-gu Ansan-si, Gyeonggi-do 15426, Republic of Korea

[§] School of Pharmacy, Sungkyunkwan University, 2066 Seobu-ro, Jangan-gu, Suwon, Gyeonggi-do 16419, Republic of Korea

^{||} Daewoong Pharmaceutical, 72 Dugye-ro, Pogok-eup, Cheoin-gu, Yongin-si, Gyeonggi-do 17028, Republic of Korea

[⊥] Department of Global Medical Science, Sungshin University, 76 Dobong-ro, Gangbuk-gu, Seoul 01133, Republic of Korea

ABSTRACT: We developed an orally active and blood-brain barrier-permeable benzofuran analogue (**8**, **MDR-1339**) with potent anti-aggregation activity. Compound **8** restored cellular viability from $A\beta$ -induced cytotoxicity but also improved the learning and memory function of AD model mice by reducing the $A\beta$ aggregates in the brains. Given the high bioavailability and brain permeability demonstrated in our pharmacokinetic studies, compound **8** will provide a novel scaffold for an $A\beta$ -aggregation inhibitor that may offer an alternative treatment for AD.

INTRODUCTION

Protein aggregation, once thought to be a rare phenomenon in living organisms, not only occurs ubiquitously but also contributes to the pathogenesis of more than 50 human diseases.¹ Though complete mechanisms of how protein aggregates are formed and how these aggregates are involved in the etiology of various diseases have not been fully understood, age-related impairment of protein quality control has been suspected as a major factor in these processes, which accounts for the fact that many disease markers found in senile disorders are protein aggregates. For example, amylin in type II diabetes, α -synuclein in Parkinson's disease, and amyloid β ($A\beta$) peptides in Alzheimer's disease (AD) form insoluble fibers or toxic soluble oligomers, which cause the loss of normal cellular function and accelerate aggregation even further.

Among these pathogenic aggregates, $A\beta$ peptides are probably the most extensively studied because they are central to the amyloid hypothesis, one of the leading theories of AD pathogenesis.² Many anti-amyloid therapies, such as β - and γ -secretase inhibitors, anti- $A\beta$ antibodies, and protein aggregation inhibitors, have been developed and tested as potential treatment options for AD. However, recent clinical trial failures cast doubt on the validity of these therapies. It has been suggested that secretase inhibitors suppress various other pathways in the brain and the peripheral tissues, exhibiting severe side effects^{3,4}; anti-

$A\beta$ antibodies might be trapped in the blood stream, allowing only limited quantities to reach the target.⁵ Despite these clinical trial failures, anti-amyloid therapies are still considered to be a promising alternative to currently available AD treatments because they have the potential to slow down or prevent neurodegeneration.⁶ Selective brain targeting with improved delivery methods may also shift the fate of the antibodies that have previously failed.^{7,8} Several long-term prevention trials and dose-adjusted clinical trials of $A\beta$ antibodies are still ongoing, and early results of these trials have suggested positive outcomes.⁹⁻¹¹

Over the past decade, many protein aggregation inhibitors have been developed as a part of anti-amyloid strategies. While several small molecules have advanced to clinical trials,^{12,13} benzofuran analogues have been extensively studied due to their high affinity and selectivity toward $A\beta$ fibrils.¹⁴⁻¹⁶ More importantly, as an alternative approach to currently developed AD therapies, recent studies have focused on multifunctional ligands and hybrid drugs.¹⁷⁻²¹ These hybrid drugs combine inhibitors of cholinesterase or antioxidants with an anti-aggregation inhibitor such as **SKF-64346 (1)**.^{22,23} While **1** is an excellent aggregation inhibitor, its *in vivo* activity and pharmacokinetic parameters have never been reported. We speculated that novel aggregation inhibitors may streamline the effort to develop highly effective therapeutic agents for AD treatment.

Therefore, we investigated a diverse series of benzofuran analogues as A β aggregation inhibitors and discovered **MDR-1339 (8)**, 2-(3,4-dimethoxyphenyl)-5-(3-methoxypropyl)benzofuran, as a clinical candidate (**Figure 1**). In this work, we aimed to determine the anti-amyloidogenic activity of compound **8** *in vitro* and *in vivo* and to assess its therapeutic effects in AD model mice. We evaluated the anti-aggregation and disaggregation properties of **8** by using preformed aggregates and soluble A β oligomers. In addition, we examined the *in vivo* activity of **8** by performing cognitive functional assays and quantifying the amounts of A β in the brains of acute and transgenic AD model mice. The anti-amyloidogenic activity of **8** was further verified by in-depth studies on pharmacokinetics and brain permeability.

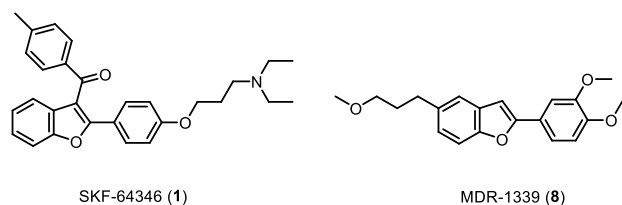
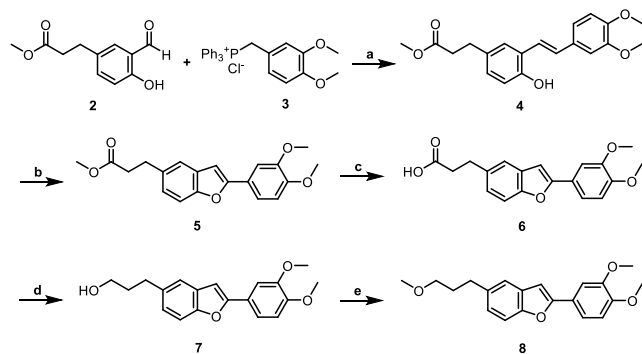


Figure 1. β -Amyloid Aggregation Inhibitors

RESULTS AND DISCUSSION

Chemistry. A highly efficient scale-up synthesis of **8** was accomplished in five steps. The Wittig reaction of 3,4-(dimethoxybenzyl)triphenylphosphonium chloride **3** with available aldehyde **2**, the oxidative intramolecular cyclization²⁴ of 2-hydroxystilbene **4** to benzofuran **5**, the basic hydrolysis of ester **5**, the reduction of acid **6** with NaBH₄, and the final methylation of **7** led to the production of target compound **8** with an overall yield of 45.4% and a purity >99%. This convenient and economical procedure is remarkably applicable for multi kilogram-scale production.

Scheme 1. Scale-up synthesis of **8**^a



^aReagents and conditions: (a) DBU, CH₃CN, r.t., 3 h; (b) I₂, K₂CO₃, THF, reflux, 4 h; (c) LiOH, MeOH-H₂O, 50 °C, 3 h; (d) (i) NaBH₄, THF, reflux, 1 h, (ii) I₂, THF, reflux, 4 h; (e) MeI, t-BuOK, THF, r.t., 2 h

In vitro activity. To determine whether **8** can inhibit the aggregation of A β monomers, we incubated monomeric A β ₁₋₄₂ solutions with **8** at different concentrations, and we quantified the amount of A β aggregates by performing Thioflavin T (ThT) assays. Because ThT generates fluorescent signals proportional to

the amount of A β fibrils, we calculated the percentage of the ThT fluorescence of each sample based on the fluorescent signals of untreated controls. We also performed the assays by using quercetin (QC), a known aggregation inhibitor, as our positive control. As shown in **Figure 2a**, **8** blocked the formation of A β aggregates in a dose-dependent manner, inhibiting the formation of A β fibrils up to 50% compared to the control. In addition, when we incubated **8** with solutions containing preformed A β aggregates, **8** appeared to disaggregate A β fibrils, reducing the amount of A β aggregates by 40% compared to that of the control (**Figure 2b**). On the basis of these observations, we believe that **8** not only blocked the formation of A β fibrils but also effectively disaggregated preformed A β aggregates. Aggregation of A β fibrils and disaggregation by compound **8** during the ThT assays was also confirmed by TEM images (**Supporting Information, Figure S1**).

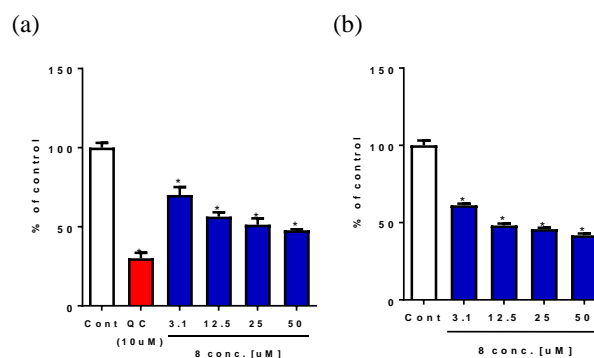


Figure 2. Effect of **8** on (a) the aggregation of monomeric A β ₁₋₄₂ and (b) the disaggregation of A β fibrils *in vitro*. ThT assays were performed by incubating 25 μ M of monomeric A β ₁₋₄₂ solutions (Fig 2a) or preformed A β aggregates (Fig 2b) with **8** at the indicated concentrations. The data are presented as the mean \pm SD from three independent experiments. One-way ANOVA, Dunnett test, [* p<0.001: vs. control]

To investigate whether **8** can protect cells from A β -induced toxicity, we carried out cytotoxicity assays using 3-(4,5-dimethylthiazol-2-yl)-2,5-diphenyltetrazolium bromide (MTT). We treated HT22 cells, a neuronal cell line derived from the mouse hippocampus, with **8** at different concentrations and subsequently incubated these cells with preformed A β aggregates. The cell viability of each sample was assessed by calculating percent values based on the changes of the signal intensity between untreated cells and A β -treated cells as a control. As shown in **Figure 3a**, the treatment of A β aggregates alone reduced the cell viability to 40% of that observed in normal cells.

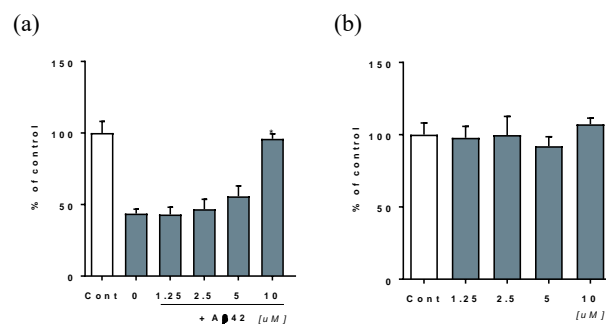


Figure 3. (a) Effect of **8** on the cell viability of the HT22 cells exposed to A β aggregates. (b) Effect of **8** on cell viability without the treatment of A β

aggregates. HT22 cells were treated with preformed A β aggregates that were prepared by using 25 μ M of monomeric A β solutions. The data were presented as the mean \pm SD from three independent experiments. One-way ANOVA, Dunnett test, [$* p < 0.001$: vs. control]

The treatment of **8** protected cells from this A β -induced toxicity in a dose-dependent manner, maintaining cell viability to normal levels at 10 μ M. We also measured the cytotoxicity of **8** in HT22 cells without A β aggregates, confirming that **8** alone did not affect cell viability at the indicated concentrations (**Figure 3b**). These results suggest that **8** suppressed the formation of toxic A β aggregates, protecting cells from A β -induced toxicity.

Next, we wanted to further verify that **8** can suppress the formation of A β aggregates. Therefore, we incubated A β aggregates with **8** and analyzed the size distribution using SDS-PAGE followed by silver staining. In addition, we also incubated A β aggregates with congo red, a diazo dye with anti-amyloidogenic activity,²⁵ as a positive control for comparison. As shown in **Figure 4**, when we started the incubation, all samples contained a mixture of monomeric, dimeric and trimeric A β peptides. After the samples were incubated for 48 h, we found that these monomeric peptides remained in both congo red- and **8**-treated samples. On the other hand, these low molecular weight bands mostly disappeared in the vehicle-treated samples, implying that they transformed into high molecular aggregates. These results suggest that **8** prevented oligomer formation of A β peptides and reduced the formation of A β fibrils to a similar extent as congo red.

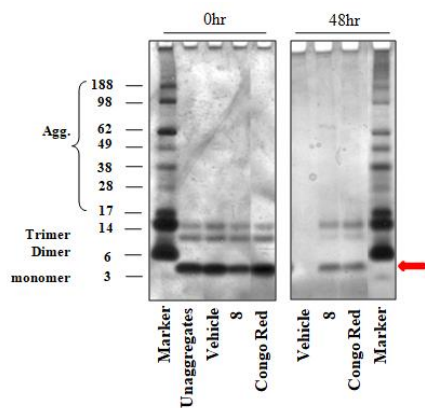


Figure 4. Effect of **8** on preformed A β aggregates.

In vivo activity. To verify the anti-amyloidogenic activity of **8**, we evaluated its efficacy in animal models of AD. First, we assessed learning and memory function in an acute AD mouse model by performing step-through passive avoidance tests. In this model, A β aggregates were directly injected into the brains of normal mice to induce acute neurotoxicity. After orally administering **8** for three consecutive days, the passive avoidance responses were evaluated by following the standard protocol.²⁶ As shown in **Figure 5a**, vehicle-treated mice demonstrated significantly reduced step-through latency (sec) due to the acute impairment of cognitive function; however, the treatment of **8** effectively restored the passive avoidance responses in a dose-dependent manner, with an ED₅₀ value of 0.19 mg/kg. Specifically, the step-through latency in the sessions with mice treated with a 10 mg/kg dose (201.2 \pm 29.4) was restored close to the control level.

In addition, we performed Y-maze tests to further verify the *in vivo* activity of **8**. As described in **Figure 5b**, vehicle-treated mice showed a significantly suppressed percentage of spontaneous alternation compared to that in normal mice, indicating severe impairments in spatial memory; however, the treatment of **8** again restored alternation behavior in a dose-dependent manner, with an ED₅₀ value of 0.18 mg/kg. More importantly, **8** appeared to fully recover the percentage of alternation at a dose of 1 mg/kg (71.22 \pm 3.14) and a dose of 10 mg/kg (73.07 \pm 2.83).

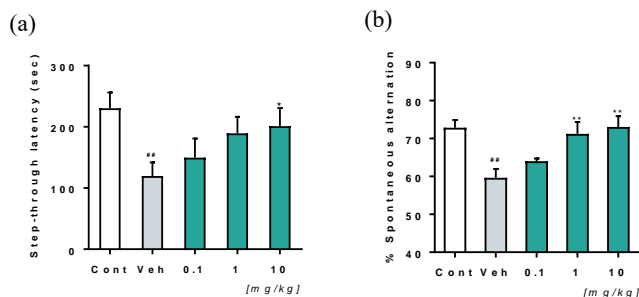


Figure 5. Behavioral effects of **8** in an acute AD model mice. (a) Passive avoidance tests to assess learning and memory impairments; (b) Y maze tests to assess spatial memory function (## $P < 0.01$ vs. Control, * $P < 0.05$, ** $P < 0.01$ vs. Vehicle)

On the basis of these observations, we decided to test **8** with a double transgenic AD mouse model, APP/PS1. In APP/PS1 mice, extracellular A β deposition can be detected at the age of 2.5 months and apparent dysfunction of learning and memory can be monitored at the age of 6 to 8 months.²⁷ While we observed the significant improvement in the Y-maze tests at the dose of 10 mg/kg in our acute AD model mice, we speculated that the double transgenic animal model might require much higher doses since they were in the further advanced state of AD. Therefore, we decided to treat 29-week-old APP/PS1 mice with **8** at doses of 30 mg/kg and 100 mg/kg for eight weeks by daily oral administration and performed Y-maze tests. As described in **Figure 6**, vehicle-treated mice demonstrated a severe reduction in the percentage of spontaneous alternation (52.64 \pm 4.15), which was even lower than the values observed for the acute AD model mice; however, the treatment with **8** significantly improved spontaneous alternation at both doses without any apparent toxicity: 63.73 \pm 1.06% for 30 mg/kg, and 63.93 \pm 2.24% for 100 mg/kg.

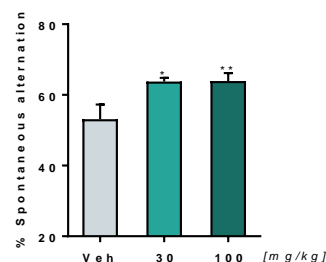


Figure 6. Y-maze tests following **8** treatment in APP/PS1 mice (* $P < 0.05$, ** $P < 0.01$ vs. Vehicle)

To confirm whether the anti-amyloidogenic activity of **8** resulted in these improvements in cognitive function in APP/PS1 mice, we quantified the levels of A β aggregates in the brain by

immunoassay. As demonstrated in **Figure 7**, when compared to the vehicle-treated mice, mice treated with **8** appeared to have dose-dependent reductions in the amounts of $A\beta_{1-40}$ and $A\beta_{1-42}$, while mice treated with 100 mg/kg had the most significant reduction of $A\beta_{1-42}$ (70% of vehicle group). We believe that these results support that **8** effectively reduced the overall amount of $A\beta$ aggregates, thus improving cognitive function in AD model mice.

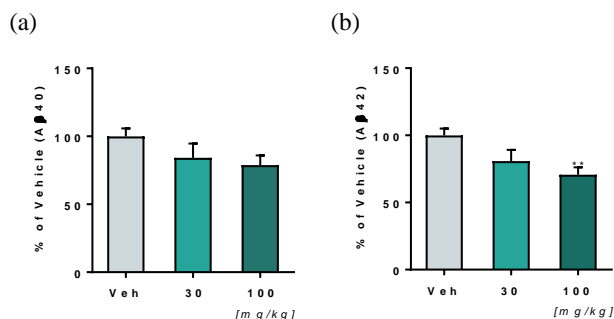


Figure 7. (a) $A\beta_{1-40}$ and (b) $A\beta_{1-42}$ levels in the brains of APP/PS1 transgenic mice treated with **8**. (** $P < 0.01$ vs. Vehicle; The brain $A\beta$ were quantified by using the antibodies specific to monomeric $A\beta$, after brain tissues were homogenized and amyloid fibrils were solubilized to monomers)

Pharmacokinetics and brain permeability. To further validate the *in vivo* activity of **8**, we determined pharmacokinetic parameters and summarized these values in **Table 1** and **Table 2**. The bioavailability of **8** increased up to 79.1% (30 mg/kg) in a dose-dependent manner, indicating that our compound is systematically well absorbed, and suitable for oral administration in mice (**Table 1**). When we administered **8** to various other species, we also observed high bioavailabilities and a relatively long half-life among rats and monkeys, which is consistent with the results from ICR mice (**Table 2**).

After confirming the high bioavailability of **8**, we evaluated the blood-brain barrier (BBB) permeability of **8** by oral administration in ICR mice over the course of nine hours. As shown in **Figure 8**, **8** demonstrated consistent brain to plasma ratio (K_p) values that ranged from 1.2 to 1.5, indicating that **8** efficiently crossed the BBB. This high bioavailability and BBB permeability again support our hypothesis that **8** effectively reduced $A\beta$ aggregates in the brains of AD mice and restored their cognitive function.

Table 1. Pharmacokinetic parameters of 8^a

PK parameters	I.V.	Oral		
	3 mg/kg	3 mg/kg	10 mg/kg	30 mg/kg
$T_{1/2}$	1.4	2.0	1.6	3.3
T_{max}	-	0.7	0.7	3.0
C_{max}	4869.9 (C_0)	101.9	660.1	1700.6
AUC_{last}	1303.5	245.6	2238.8	10429.5
AUC_{inf}	1325.1	283.1	2293.8	10475.7
BA	-	21.4	51.9	79.1

^a AUC_{inf} , total area under the plasma concentration time curve from time zero to time infinity ($hr \cdot ng/mL$); AUC_{last} , total area under the plasma concentration time curve from time zero to the last measured time ($hr \cdot ng/mL$); C_{max} , peak plasma concentration (ng/mL); $T_{1/2}$, terminal half-life (hr); T_{max} , time to reach C_{max} (hr); BA, bioavailability (%).

Table 2. Pharmacokinetic parameters of 8 in rat, dog, monkey and mouse.^a

Species	I.V. Oral						
	Cl	V_{ss}	$T_{1/2}$	C_{max}	AUC	$T_{1/2}$	F
Rat	33	10	3.4	421	4203	3.8	51
Dog	29	2.7	1.1	1607	4186	1.4	25
Monkey	7	3.8	12.9	969	13747	12.9	70
Mouse	10.5	2.5	2.75	944	13178	5.87	83.3

^a AUC , area under curve($ng \cdot h / mL$); C_{max} , maximum concentration (ng/mL); $T_{1/2}$, half-life (h); T_{max} , time to reach C_{max} ; CL, time-averaged total body clearance ($mL/min/kg$); V_{ss} , apparent volume of distribution at steady state (L/kg); F, bioavailability(%).

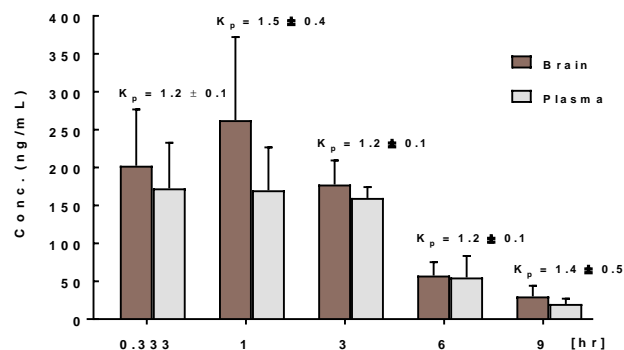


Figure 8. Blood-brain barrier permeability of **8**. ICR mice ($n=3$) were orally administered 10 mg/kg of **8**. K_p indicates AUC_{brain}/AUC_{plasma}

Cytochrome P450 (CYP) inhibition. To evaluate the toxicity profile of **8**, we determined the inhibition of cytochrome P450 using the human liver microsome. As shown in **Table 3**, **8** did not significantly inhibit a panel of CYP isozymes, while it slightly inhibited CYP2C8 ($IC_{50} = 31.4 \mu M$). This result suggests that **8** is unlikely to cause drug-drug interactions via metabolism.

Table 3. Human CYP inhibition of 8

CYP450	1A2	2A6	2C8	2C9	2C19	2D6	3A4
IC_{50} (μM)	>50	>50	31.4	>50	>50	>50	>50

CONCLUSION

In this work, we developed an orally active and BBB-permeable $A\beta$ aggregation inhibitor as a potential therapeutic option for Alzheimer's disease. Compound **8** demonstrated

anti-amyloidogenic activity against preformed A β aggregates and soluble oligomers *in vitro*. Compound **1** also protected neuronal cells from A β -induced cytotoxicity in a dose-dependent manner. To further validate the anti-amyloidogenic activity, **8** was orally administered to AD model mice, and it restored learning and memory function to a level close to that of the control without any apparent toxicity. When we examined the amounts of brain A β aggregates in these AD mice, **8** significantly reduced the amount of A β ₁₋₄₂ aggregates, suggesting that the anti-amyloidogenic activity of **8** improved the cognitive function of AD model mice. In addition, pharmacokinetic parameters indicated that **8** has high oral bioavailability in mice, rats, and monkeys and also showed consistently high brain to plasma ratio (Kp) values over the course of nine hours. Taken together, these results suggest that **8** is a highly effective A β aggregation inhibitor with excellent bioavailability and brain permeability, and it is currently under clinical development. We believe that inongoing clinical phase I study, **8** will provide a novel scaffold for an A β aggregation inhibitor that may offer a promising alternative treatment for AD in the near future.

EXPERIMENTAL SECTION

General Methods. ¹H and ¹³C NMR spectra were recorded on a Bruker Analytik, DE/AVANCE Digital 500 at 500 and 125 MHz. Mass spectra were recorded on a VG Trio-2 GC-MS instrument and a 6460 Triple Quad LC-MS instrument. All final compounds were purified to >95% purity, as determined by high-performance liquid chromatography (HPLC). HPLC was performed on an Agilent 1120 Compact LC (G4288A) instrument using an Agilent TC-C18 column (4.6 mm \times 250 mm, 5 μ m).

Methyl 3-(3-(3,4-dimethoxy-styryl)-4-hydroxyphenyl) propanoate (4). 3,4-dimethoxybenzylchloride (155.8 kg), triphenylphosphine (203.8 kg), and sodium iodide (89.6 kg) were placed in the first reactor, and then, acetonitrile (655 L) was added. The resulting mixture was heated to reflux at 75-85 °C for 2 h to terminate the reaction. The reaction solution was cooled to ambient temperature. Then, methyl 3-(3-formyl-4-hydroxyphenyl)propanoate (**2**) (131 kg) was placed in a second reactor, and acetonitrile (655 L) was added. The resulting mixture was stirred at room temperature, and then, 1,8-diazabicyclo[5.4.0]-7-undecene (DBU, 114.9 kg) was added. Next, the (3,4-dimethoxybenzyl)triphenylphosphonium chloride (**3**) prepared in the first reactor was added dropwise into the second reactor for 30 min. After 3 h, the reaction was terminated. The reaction solution was cooled to room temperature and concentrated under reduced pressure. The concentrate was dissolved in ethylacetate (1400 L) and stirred with the addition of water (1270 L). The organic layer was separated, dehydrated with MgSO₄ (40 kg), and concentrated under reduced pressure. The concentrate was cooled to room temperature, dissolved in ethylacetate (400 L), and crystallized by adding n-hexane (400 L). Stirring was performed at room temperature for 2 h, and the crystals were filtered, washed with ethylacetate/n-hexane = 1/3 (65.5 L), and dried in a vacuum at 40 °C, yielding **4** (326.6 kg, 75.8% yield). ¹H NMR (CDCl₃, 500 MHz) δ 7.39 (s, 1H), 7.32-6.85 (m, 5H), 6.78 (d, 1H, *J* = 8.20 Hz), 3.98 (s, 3H), 3.94 (s, 3H), 3.72 (s, 3H), 2.95 (t, 2H, *J* = 7.40 Hz), 2.68 (t, 2H, *J* = 8.00 Hz).

Methyl 3-(2-(3,4-dimethoxyphenyl)benzofuran-5-yl)propanoate (5). Iodine (359.7 kg) was added to **4** (323.5 kg) in THF (1600 L) and K₂CO₃ (391.7 kg) was added. The mixture was refluxed. After 4 h, the mixture was concentrated *in vacuo* and dissolved in ethylacetate (1600 L). A saturated Na₂S₂O₃ solution (Na₂S₂O₃ 140 kg/water 1000 L) was added to the mixture and stirred for 10 min. The organic compound was extracted with ethylacetate and dried over MgSO₄ (40 kg) and concentrated *in vacuo* (40-50 °C). The concentrate was dissolved in dichloromethane (300 L) and crystallized by adding MeOH (300 L). Stirring was performed at room temperature for 2 h, and the crystals were filtered, washed with MeOH (32 L), and dried at 40 °C over 12 h, yielding **5** (125.4 kg, 78% yield, >95% purity). ¹H NMR (CDCl₃, 500 MHz) δ 7.48-7.43 (m, 4H), 7.13 (dd, 1H, *J* = 8.40 Hz, 2.10 Hz), 6.97 (d, 1H, *J* = 8.40 Hz), 6.89 (s, 1H), 4.30 (s, 3H), 3.97 (s, 3H), 3.73 (s, 3H), 3.09 (t, 2H, *J* = 7.60 Hz), 2.73 (t, 2H, *J* = 7.70 Hz).

3-(2-(3,4-Dimethoxyphenyl)benzofuran-5-yl)propanoic acid (6). LiOH·H₂O (13.6 kg) was dissolved in water (385 L) and it was added to compound **5** (55 kg) in MeOH (440 L) and refluxed for 3 h. The mixture was allowed to cooled to ambient temperature, acidified to pH 2.0-3.0 with 6 N HCl. The solution was stirred at room temperature for 30 min and at 0-5 °C for 1 h. Crystallized product was filtered, washed with water (55 L), and dried at 60 °C over 24 h, yielding **6** (52.2 kg, 99% yield, >99% purity). ¹H NMR (CDCl₃, 500 MHz) δ 12.03 (s, 1H), 7.49-7.40 (m, 4H), 7.15 (dd, 1H, *J* = 8.30 Hz, 2.00 Hz), 6.98 (d, 1H, 8.30 Hz), 6.89 (s, 1H), 4.30 (s, 3H), 4.00 (s, 3H), 3.10 (t, 2H, *J* = 7.70 Hz), 2.78 (t, 2H, *J* = 8.10 Hz).

3-(2-(3,4-Dimethoxyphenyl)benzofuran-5-yl)propan-1-ol (7). NaBH₄ (12.1 kg) and THF (364 L) were placed in a reactor and stirred. **6** (52 kg) was slowly added (generation of H₂ gas) to the mixture, THF (26 L) was added, and the resulting mixture was heated to reflux at 65-75 °C for 1 h. The reaction solution was cooled to 30-40 °C, and I₂ (28.3 kg) and THF (26 L) were added. The reaction solution was heated to reflux to 65-75 °C for 4 h, and the reaction was terminated. The reaction solution was cooled to 10-15 °C, and ethylacetate (364 L) was added. Water (364 L) was added while paying attention to gas generation. The pH of the solution was adjusted to 3.0-4.0 using 6 N HCl. The layers were separated; the organic layer was stored, and ethylacetate (104 L) was added to the water layer. After layer separation, the water layer was discarded, and the organic layer was combined with the stored organic layer. The organic layer was washed with 10% NaHSO₃ (NaHSO₃ 36.4 kg/water 364 L), dehydrated with MgSO₄ (26 kg), and washed with ethylacetate (52 L). The reaction solution was concentrated under reduced pressure at 40-50 °C, and isopropylalcohol (260 L) was added to the concentrate, heated to 70-80 °C and dissolved. Next, the concentrate was slowly cooled to 20-25 °C, thus producing crystals. Stirring was performed at 20-25 °C for 2 h, and the crystals were filtered, washed with 52 L of isopropylalcohol, and dried at 40 °C for 12 h or longer, yielding **7** (42 kg, 84.3% yield, >99% purity). ¹H NMR (CDCl₃, 500 MHz) δ 7.48-7.40 (m, 4H), 7.10 (dd, 1H, *J* = 8.40 Hz, 2.10 Hz), 6.96 (d, 1H, *J* = 8.40 Hz), 6.85 (s, 1H), 4.30 (s, 3H), 4.00 (s, 3H), 3.74 (t, 2H, *J* = 6.40 Hz), 2.84 (t, 2H, *J* = 7.30 Hz), 1.99 (q, 2H, *J* = 6.40 Hz), 1.71 (s, 1H).

2-(3,4-Dimethoxyphenyl)-5-(3-methoxypropyl)benzofuran (8). t-BuOK (76.3 kg) and THF (594 L) were placed in a reactor and stirred. **7** (84.9 kg) was added, and then, THF (84.9 L) was added. The resulting solution was cooled to 10-15 °C, and MeI

(50.8 L) was added at 30 °C or less. The reaction solution was stirred at 20–25 °C for 2 h, and the reaction was subsequently terminated. The reaction solution was cooled to 10–15 °C, and ethylacetate (594 L) was added. Water (594 L) was added while paying attention to gas generation. The pH of the solution was adjusted to 3.0–4.0 using 6 N HCl. After layer separation, the organic layer was stored, and ethylacetate (170 L) was added to the water layer. After a subsequent layer separation, the water layer was discarded, and the organic layer was combined with the stored organic layer. The organic layer was washed with 10% NaHSO₃ (NaHSO₃ 59.4 kg/water 594 L), dehydrated with MgSO₄ (42.5 kg) and washed with ethylacetate (84.9 L). The reaction solution was concentrated under reduced pressure at 40–50 °C. EtOH (424.5 L) was added to the concentrate. The concentrate was heated to 70–80 °C and dissolved. Next, the concentrate was slowly cooled to 20–25 °C, thus producing crystals. Stirring was performed at 20–25 °C for 2 h, and the crystals were filtered, washed with EtOH (84.9 L), and dried at 40 °C for 8 h or longer, yielding **8** (81.7 kg, 92.1% yield, >99% purity) as a white solid. mp = 101–105 °C. ¹H NMR (CDCl₃, 500 MHz) δ 7.48–7.32 (m, 4H), 7.09 (d, 1H, *J* = 8.50 Hz), 6.94 (d, 1H, *J* = 8.00 Hz), 6.85 (s, 1H), 3.99 (s, 3H), 3.93 (s, 3H), 3.41 (t, 2H, *J* = 5.50 Hz), 3.36 (s, 3H), 2.78 (t, 2H, *J* = 7.50 Hz), 1.94 (t, 2H, *J* = 7.00 Hz). ¹³C NMR (200 MHz, CDCl₃) δ 156.1, 153.3, 149.4, 149.1, 136.5, 129.5, 124.5, 123.6, 119.9, 117.8, 111.3, 110.6, 108.0, 99.8, 71.9, 58.5, 55.9, 32.2, 22.6, 14.1. MS(FAB) *m/z* 327 [M+H]⁺. HRMS(FAB) calc. for C₂₀H₂₂O₄ [M+H]⁺ 327.1591, found 327.1594.

■ ASSOCIATED CONTENT

Supporting Information. The Supporting Information is available free of charge on the ACS Publication website at DOI: Detailed experimental procedures for *in vitro* assays and *in vivo* animal studies, and molecular formula strings.

■ AUTHOR INFORMATION

Corresponding Author

* Phone, 82-2-880-7846; E-mail, jeewoo@snu.ac.kr.

Notes

The authors declare no competing financial interest.

■ ACKNOWLEDGMENT

This study was supported by a grant (H11C0918) of the Korea Technology R&D Project, Ministry of Health & Welfare, Republic of Korea and partly Cooperative Research Program for Agriculture Science & Technology Development (PJ00910303) by RDA.

■ ABBREVIATIONS

Aβ, β-amyloid; AD, Alzheimer's disease; ThT, thioflavin T; MTT, 3-(4,5-dimethylthiazol-2-yl)-2,5-diphenyltetrazolium bromide; SDS-PAGE, sodium dodecyl sulfate-polyacrylamide gel electrophoresis; BBB, blood-brain barrier; CYP, cytochrome P450

■ REFERENCES

(1) Knowles, T. P.; Vendruscolo, M.; Dobson, C. M. The amyloid state and its association with protein misfolding diseases. *Nat. Rev. Mol. Cell Biol.* **2014**, *15*, 384–396.

(2) Hardy, J.; Selkoe, D. J. The amyloid hypothesis of alzheimer's disease: Progress and problems on the road to therapeutics. *Science* **2002**, *297*, 353–356.

(3) Berk, C.; Sabbagh, M. N. Successes and failures for drugs in late-stage development for alzheimer's disease. *Drugs Aging* **2013**, *30*, 783–792.

(4) De Strooper, B. Lessons from a failed gamma-secretase alzheimer trial. *Cell* **2014**, *159*, 721–726.

(5) Yu, Y. J.; Watts, R. J. Developing therapeutic antibodies for neurodegenerative disease. *Neurotherapeutics* **2013**, *10*, 459–472.

(6) Mullard, A. Alzheimer amyloid hypothesis lives on. *Nat. Rev. Drug Discovery* **2016**, *16*, 3–5.

(7) Saraiva, C.; Praca, C.; Ferreira, R.; Santos, T.; Ferreira, L.; Bernardino, L. Nanoparticle-mediated brain drug delivery: Overcoming blood-brain barrier to treat neurodegenerative diseases. *J. Controlled Release* **2016**, *235*, 34–47.

(8) Neves, V.; Aires-da-Silva, F.; Corte-Real, S.; Castanho, M. A. Antibody approaches to treat brain diseases. *Trends Biotechnol.* **2016**, *34*, 36–48.

(9) Mullard, A. Sting of alzheimer's failures offset by upcoming prevention trials. *Nat. Rev. Drug Discovery* **2012**, *11*, 657–660.

(10) Reardon, S. Antibody drugs for alzheimer's show glimmers of promise. *Nature* **2015**, *523*, 509–510.

(11) Sevigny, J.; Chiao, P.; Bussiere, T.; Weinreb, P. H.; Williams, L.; Maier, M.; Dunstan, R.; Salloway, S.; Chen, T.; Ling, Y.; O'Gorman, J.; Qian, F.; Arastu, M.; Li, M.; Chollate, S.; Brennan, M. S.; Quintero-Monzon, O.; Scannevin, R. H.; Arnold, H. M.; Engber, T.; Rhodes, K.; Ferrero, J.; Hang, Y.; Mikulskis, A.; Grimm, J.; Hock, C.; Nitsch, R. M.; Sandrock, A. The antibody aducanumab reduces abeta plaques in alzheimer's disease. *Nature* **2016**, *537*, 50–56.

(12) Cheng, B.; Gong, H.; Xiao, H.; Petersen, R. B.; Zheng, L.; Huang, K. Inhibiting toxic aggregation of amyloidogenic proteins: A therapeutic strategy for protein misfolding diseases. *Biochim. Biophys. Acta* **2013**, *1830*, 4860–4871.

(13) Eisele, Y. S.; Monteiro, C.; Fearn, C.; Encalada, S. E.; Wiseman, R. L.; Powers, E. T.; Kelly, J. W. Targeting protein aggregation for the treatment of degenerative diseases. *Nat. Rev. Drug Discovery* **2015**, *14*, 759–780.

(14) Howlett, D. R.; Perry, A. E.; Godfrey, F.; Swatton, J. E.; Jennings, K. H.; Spitzfaden, C.; Wadsworth, H.; Wood, S. J.; Markwell, R. E. Inhibition of fibril formation in beta-amyloid peptide by a novel series of benzofurans. *Biochem. J.* **1999**, *340* (Pt 1), 283–289.

(15) Ono, M.; Kawashima, H.; Nonaka, A.; Kawai, T.; Haratake, M.; Mori, H.; Kung, M. P.; Kung, H. F.; Saji, H.; Nakayama, M. Novel benzofuran derivatives for pet imaging of beta-amyloid plaques in alzheimer's disease brains. *J. Med. Chem.* **2006**, *49*, 2725–2730.

(16) Hayne, D. J.; Lim, S.; Donnelly, P. S. Metal complexes designed to bind to amyloid-β for the diagnosis and treatment of alzheimer's disease. *Chem. Soc. Rev.* **2014**, *43*, 6701–6715.

(17) Bajda, M.; Guzior, N.; Ignasik, M.; Malawska, B. Multi-target-directed ligands in alzheimer's disease treatment. *Curr. Med. Chem.* **2011**, *18*, 4949–4975.

(18) Leon, R.; Garcia, A. G.; Marco-Contelles, J. Recent advances in the multitarget-directed ligands approach for the treatment of alzheimer's disease. *Med. Res. Rev.* **2013**, *33*, 139–189.

(19) Dias, K. S.; Viegas, C., Jr. Multi-target directed drugs: A modern approach for design of new drugs for the treatment of alzheimer's disease. *Curr. Neuropharmacol.* **2014**, *12*, 239–255.

(20) Unzeta, M.; Esteban, G.; Bolea, I.; Fogel, W. A.; Ramsay, R. R.; Youdim, M. B.; Tipton, K. F.; Marco-Contelles, J. Multi-target directed donepezil-like ligands for alzheimer's disease. *Front. Neurosci.* **2016**, *10*, 205.

(21) Prati, F.; Cavalli, A.; Bolognesi, M. L. Navigating the chemical space of multitarget-directed ligands: From hybrids to fragments in alzheimer's disease. *Molecules* **2016**, *21*, 466.

(22) Rizzo, S.; Riviere, C.; Piazzini, L.; Bisi, A.; Gobbi, S.; Bartolini, M.; Andrisano, V.; Morrioni, F.; Tarozzi, A.; Monti, J. P.; Rampa, A. Benzofuran-based hybrid compounds for the inhibition of cholinesterase activity, beta amyloid aggregation, and abeta neurotoxicity. *J. Med. Chem.* **2008**, *51*, 2883-2886.

(23) Rizzo, S.; Tarozzi, A.; Bartolini, M.; Da Costa, G.; Bisi, A.; Gobbi, S.; Belluti, F.; Ligresti, A.; Allara, M.; Monti, J. P.; Andrisano, V.; Di Marzo, V.; Hrelia, P.; Rampa, A. 2-arylbenzofuran-based molecules as multipotent alzheimer's disease modifying agents. *Eur. J. Med. Chem.* **2012**, *58*, 519-532.

(24) Pan, C.; Yu, J.; Zhou, Y.; Wang, Z.; Zhou, M.-M. An efficient method to synthesize benzofurans and naphthofurans. *Synlett* **2006**, *11*, 1657-1662.

(25) Lorenzo, A.; Yankner, B. A. Beta-amyloid neurotoxicity requires fibril formation and is inhibited by congo red. *Proc. Natl. Acad. Sci.* **1994**, *91*, 12243-12247.

(26) Song, D. K.; Won, M. H.; Jung, J. S.; Lee, J. C.; Kang, T. C.; Suh, H. W.; Huh, S. O.; Paek, S. H.; Kim, Y. H.; Kim, S. H. Behavioral and neuropathologic changes induced by central injection of carboxyl-terminal fragment of β -amyloid precursor protein in mice. *J. Neurochem.* **1998**, *71*, 875-878.

(27) Cheng, S.; LeBlanc, K. J.; Li, L. Triptolide preserves cognitive function and reduces neuropathology in a mouse model of alzheimer's disease. *PLoS One* **2014**, *9*, e108845.

Table of Contents (TOC) graphic

